Fabrication of poly (vinylidene fluoride) films by ultrasonic spray coating; uniformity and piezoelectric properties

Taleb, Sepide; Badillo-Ávila, Miguel A.; Acuautla, Mónica

Published in:
Materials & design

DOI:
10.1016/j.matdes.2021.110273

Publication date:
2021

Materials & Design 212 (2021) 110273

Contents lists available at ScienceDirect

Materials & Design

journal homepage: www.elsevier.com/locate/matdes

Fabrication of poly (vinylidene fluoride) films by ultrasonic spray coating; uniformity and piezoelectric properties

Sepide Taleb, Miguel A. Badillo-Ávila, Mónica Acuautla *

Faculty of Science and Engineering, University of Groningen, Nijenborgh 4, 9747AG Groningen, the Netherlands

HIGHLIGHTS

- Ultrasonic spray coating system is used for fabrication of pure PVDF films with high piezoelectric coefficient (d_{33} = 48 pm/V).
- Highly crystalline (56%) PVDF films with predominant β phase for flexible and transparent engineering devices are achieved without post processing.
- Uniformity and roughness (<50 nm) of the PVDF films strongly affects their piezoelectric properties.
- We proved that the ultrasonic spray coating method is capable of producing large-scale, low-cost PVDF films in a single step.

GRAPHICAL ABSTRACT

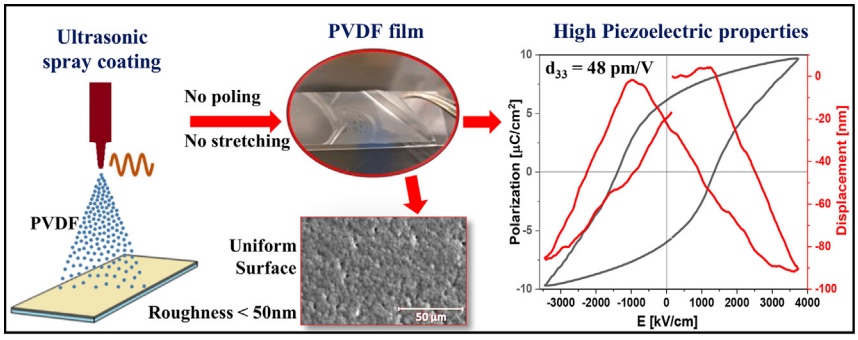

ARTICLE INFO

Article history:
Received 1 September 2021
Revised 19 November 2021
Accepted 22 November 2021
Available online 23 November 2021

Keywords:
Poly (vinylidene fluoride) (PVDF)
Ultrasonic spray coating
Piezoelectric coefficient
Uniformity

ABSTRACT

Piezoelectric Poly (vinylidene fluoride) (PVDF) films with high flexibility are a suitable and promising replacement for rigid ceramic piezoelectric materials. However, for this purpose, enhancing piezoelectric properties and adopting an industrial fabrication method are of great importance. In this study, 5–9 μm thick PVDF films were fabricated by a nozzle-less ultrasonic spray coating (USC) system, followed by an annealing process at 100 °C. By applying proper spraying parameters, we could obtain highly uniform films with large d_{33} values (48 pm/V) and 56% crystallinity. Results show that the uniformity of the films plays an important role in the final piezoelectric properties. Thus, ultrasonic spray coating method can be used for fabrication of large-scale piezoelectric films with no need for poling or stretching processes.

1. Introduction

Since 1969, when PVDF was discovered as an organic piezoelectric material [1], a wide variety of research has been done on piezoelectric PVDF films. The outstanding mechanical properties of PVDF as a lead-free material, in comparison to inorganic piezoelectric single crystals and ceramics, have drawn the attention of many researchers [1–4]. Their focus has been mostly on polymer chain structure [5], fabrication methods [6,7], piezoelectric properties [2], mechanical strength [8], and sensor/actuator/energy harvesting applications [1,3,4,9]. However, the application of piezoelectric PVDF films is not limited to the mentioned fields and is spreading rapidly to the new disciplines. For instance, ferroelectric PVDF-TrFE films have been recently used in nano electric devices such as non-volatile memories [10], photodetectors [11], field-effect transistors [12], and PVDF composites are used for electric accessories and embedded capacitors [13]. Therefore, seeking a reliable and simple method for industrial fabrication of these piezoelectric films is of great importance.

* Corresponding author.
E-mail addresses: s.taleb@rug.nl (S. Taleb), m.a.badillo.avila@rug.nl (M.A. Badillo-Ávila), m.i.acuautla.meneses@rug.nl (M. Acuautla).

https://doi.org/10.1016/j.matdes.2021.110273
0264-1275/

PVDF is a semi-crystalline material with crystalline regions embedded in an amorphous matrix [1]. This material can be crystallized into five different phases including all-trans planar zigzag β (TTTT, form I) phase, α phase (TGTG', form II), γ phase (T3GT3G', form III), δ phase (TGTG'), and ε phase (T3GT3G') [14,15]. Among these, α and ε are non-polar due to the antiparallel packing of the dipoles within the unit cell [15], while β and γ phases are electrically active (polar). Usually, the films formed directly from the melt possess the α phase, and stretching, poling or quenching is required to convert their nonpolar phase to polar phase [16–18,6].

The most common methods for fabricating PVDF films are casting [18,19], spin coating [6,20], and electrospinning [7,21]. However, electrospray deposition (ESD) [22] and spray coating [23] methods can also be found in the literature. In spin coating and casting methods, the deposited film usually needs post-processing in the form of stretching, poling or quenching to achieve a polar phase. Therefore, they are not capable of large-scale fabrication. In addition, some of the post-processing such as stretching cannot be done without peeling off the film or are limited by the substrate material, while in most applications it is better to deposit the film on the final substrate to have better adhesion and quality. Electrospinning method guarantees already poled PVDF films. Nevertheless, the polarization direction is in-plane and the roughness and porosity of the films are relatively high since they are made of fibers [7].

In the electrospray deposition (ESD) method, the solution is sprayed on the substrate. Applied electric current between tip and grounded substrate leads to alignment of dipoles and provides a single-step production of PVDF films [22]. In research by Rietveld et al, thin PVDF films (400 nm) were made by the ESD method, and high d_{33} values (43 pm/V) and permanent polarization (~80 mC/m^2) were obtained by poling at a single position with the AFM tip [22]. Moreover, in [24], Hwangbo et al. reported PVDF films with a high β phase percentage of 87% fabricated using the ESD method. In Hwangbo's research, higher β phase crystallinity has been achieved by addition of ~1.3 wt% Mg $(NO_3)_2{\cdot}6H_2O$ hydrolat salt in the solution. However, neither strain nor hysteresis loops are provided in the paper.

Finally, the spray coating approach can also be used for the fabrication of PVDF films. In [23], in-situ sprayed, annealed and corona poled PVDF-TrFE films were fabricated to be used as sensors/actuators in structural health monitoring applications. After spraying the PVDF solution, the film was annealed at 120 °C. Afterwards, corona poling at 1.75 kV/μm for 5 cycles generates highly crystallized piezoelectric films with d_{33} value of ~19.4 pm/V at the frequency range of 50 kHz to 1 MHz. These films are applicable as guided wave-based structural health monitoring. In [25], 10 wt% PVDF solution was sprayed on a conductive polymer (PEDOT:PSS) coated PET substrate at 70 °C. As a result, smooth, uniform, 220 nm films with good adhesion were achieved with high β phase content (70%) besides α and γ phases. The performance of the film as an energy harvester was studied by applying 34 N force and reading an output peak-to-peak voltage of 280 mV, but no further information of the piezoelectric properties is provided. Additionally, Takise et al. [26] used various solvents to spray coat PVDF followed by corona poling, which resulted in films with a maximum d_{33} value of −12 pC/N. Afterwards, the solution was used for covering a 3D helical spring, and by compressing the spring an output voltage of −12 mV was produced. 3D printing of piezoelectric polymer materials can also provide a simpler and faster solution as an additive fabrication method [27]. However, the piezoelectric coefficient of the films made by this technique are in the range of 10–18 pm/V [28–30].

Overall, both electrospray deposition and spray coating methods provide advantages such as low-cost equipment, good thickness uniformity over large areas, and fast processing. However, the addition of ultrasonic technology can add to these benefits. The ultrasonic spray coating system is now being increasingly used as a trustworthy method in various industries such as electronics [31,32], advanced energy technology (solar [33] and fuel cells [34], biomedical devices [35,36], glass production [37], textiles [38], and the food industry [39]. The advantage of this system over conventional spray systems is the enhanced uniformity of the final film due to the atomization of the liquid and formation of smaller droplets provided by the mechanical vibration [40]. The flexibility of the system, also allows us to fabricate devices with complex designs, shapes and to use different substrates materials. Thus, expanding its application to new smart technologies.

In the present paper, we study the fabrication of freestanding PVDF films with enhanced piezoelectric properties via a nozzle-less ultrasonic spray coating system without poling. To the best of our knowledge, the only research using ultrasonic spray coating systems to fabricate a 140 μm thick PVDF film on ITO coated glass was done in 2019 by Wang et al. [41], where properties were studied by piezoresponse force microscopy.

Nozzle-less ultrasonic spray coating system provides more uniformity of layers by producing wide air pressure to the tip. The results of our research indicate that 5 μm thick PVDF films with high d_{33} value of 48 pm/V can be fabricated. The possibility of making such films on a large scale by this fabrication method paves the way for utilizing piezoelectric polymers in fabrication of practical, wearable and biocompatible sensors, energy harvesters, and flexible electronics.

2. Materials and methods

Poly (vinylidene fluoride) powder (average Mw ~534,000 by GPC), N, N-dimethylformamide (anhydrous, 99.8%) (DMF), and absolute acetone were purchased from Sigma Aldrich and used without any purification or modification. Two different PVDF solutions were prepared to study the effect of the solvent on the properties of the fabricated films. For the first solution, PVDF powder (2 g) was added to DMF solvent (40 ml) to make a 5 wt% solution. The solution was mixed using a magnetic stirrer for 2 h at 60 °C [42]. For the second solution, DMF/Acetone (70/30) was used as a solvent and the solution was mixed at 50 °C to avoid evaporation of acetone. Other steps were similar to the first solution.

2.1. Fabrication of PVDF films

A nozzle-less ultrasonic spray coating (USC) system (PRISM-400-BT) was used to make 5 and 9 μm thick piezo-polymer films. This equipment allowed us to control various parameters such as air pressure, solution flowrate, tip distance, substrate temperature, and so forth.

In the USC system, the solution was injected through a whip line to the spray head, where ultrasonication helped to atomize the liquid, while the air pressure directed the liquid droplets to a hot bench at 50 °C (Fig. 1). Clean glass substrates of size 75 mm × 25 mm were put on the hot bench, and PVDF solution was sprayed on the glass at different flowrates in a serpentine path to cover the surface completely. Several layers were deposited to obtain the intended thickness. Considering a specific flowrate, the thickness of the sample has an almost linear relationship with the number of layers. It is also clear that by increasing the flowrate, the thickness of each layer will increase subsequently. The air pressure for directing the droplets during the deposition was 30 psi. After deposition, to evaporate the remnant solvent and to enhance the crystallization of PVDF, the samples were annealed at 100 °C on a hotplate for 30 min. Afterwards, PVDF films, as shown in Fig. 2, were peeled off from the glass substrate, cut into smaller pieces,

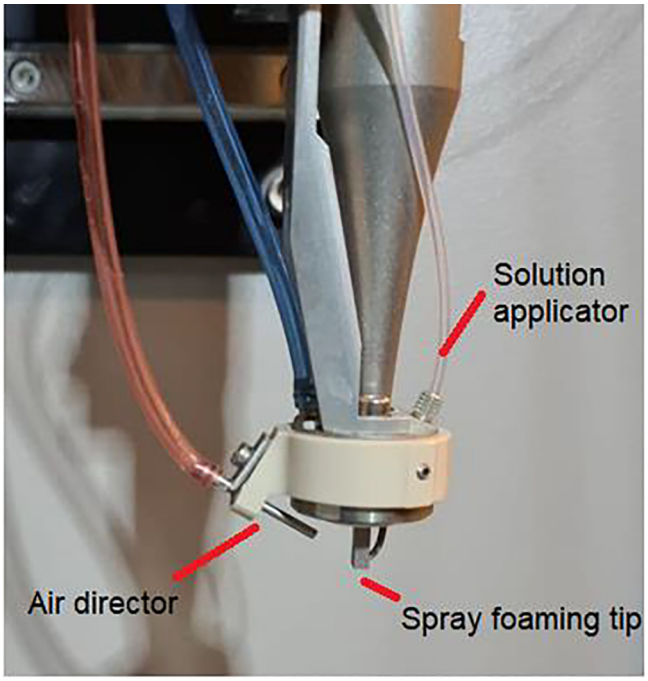

Fig. 1. Nozzle-less ultrasonic spray coating system head.

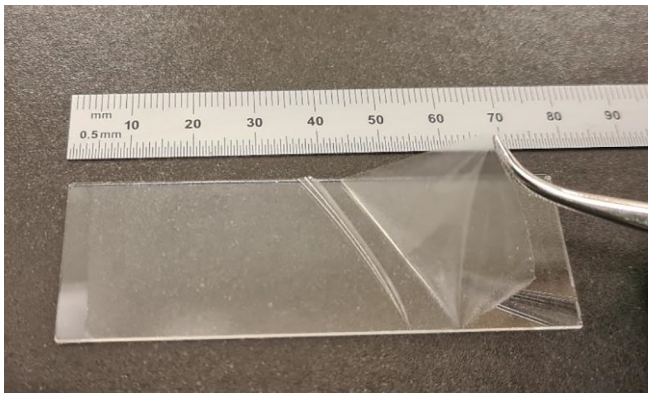

Fig. 2. A PVDF film made by USC method.

and wherever needed, top and bottom electrodes were added using silver paste.

To study the effect of solvent, flowrate, and ultrasonication, 9 μm thick samples with different conditions were fabricated using the parameters shown in Table 1. At least three different samples were made in each condition to study reproducibility and repeatability. For conditions C3 and C4, addition of acetone to the solvent increased the solvent evaporation rate due to its low boiling point. As expected, the thickness of each layer decreased by reducing the flowrate. Therefore, the samples in condition C4 were fabricated with more layers to obtain the same thickness as the other conditions.

2.2. Characterization

The thickness of the films was measured using a profilometer (Veeco Dektak 150 Surface Profiler). Polarization hysteresis and strain loops were measured at room temperature by applying an electric field up to 2500 kV/cm at a frequency of 5 Hz by a state-of-the-art aixACCT TF Analyzer 2000 ferroelectric-piezoelectric tester system. For the piezoelectric characterization, individual samples of 1x1 cm^2 were cut from large films, and top and bottom electrodes of ~2 mm^2 were added by using silver paste. In order to study the crystalline phase of PVDF films, Grazing Incidence X-ray diffraction (GIXRD) measurements were performed by Panalytical Expert Pro MRD. In addition, differential scanning calorimetry (DSC) studies were performed using a TA Instruments DSC SDT 2960, to investigate the crystalline phase and percentage of crystallinity in polymer films. For this purpose, samples with an approximate weight of 5 mg were heated at 10 °C/min from 35 °C to 300 °C under 100 ml/min argon flow. The samples were kept at 300 °C for 10 min and subsequently cooled down to room temperature at rate of 5 °C/min. Furthermore, a FEI NovaNano SEM 650 scanning electron microscope (SEM) at an accelerating voltage of 10 kV, and a Bruker's dimension icon atomic force microscopy (AFM) system were used to study the morphology of the films. Due to the high electrical resistance of polymer films, all the samples were coated with 4 nm gold before getting SEM images.

3. Results and discussion

3.1. Piezoelectric properties of films

Fig. 3 presents polarization versus electric field hysteresis loops, and Fig. 4(a–d) shows the corresponding strain loops, implementing the displacement versus the applied voltage for each condition.

The saturation polarization (P_s), remnant polarization (P_r), piezoelectric constant (d_{33}) and coercive field (E_c) were measured for several test samples, and the average results are presented in Table 2:

As shown in Table 2, the coercive field with an average value of ~1200 kV/cm did not change significantly between different fabrication conditions. In addition, the saturation polarization (~8.4 μC/cm^2) and remnant polarization (~10 μC/cm^2) in the first three conditions were almost the same. It was observed that samples fabricated at a lower flowrate (C4) improved their polarization since both saturation and remnant polarization increased. The increase in the polarization represents higher number of oriented dipoles in the film, leading to a higher d_{33} value.

One of the most important parameters for engineering applications that directly affects the transducer performance is the d_{33} piezoelectric coefficient which is measured by thickness change of the film induced by an out-of-plane electric field [43]. Based on the results in Table 2, ultrasonication increased the d_{33} value from 23 to 31 pm/V (C1 and C2), while the addition of acetone in the solvent (C2 and C3) did not considerably affect the d_{33} value.

Table 1
Various conditions of solution and deposition of samples.

Condition	Solvent	Flowrate (ml/min)	Ultrasonication	No. of layers	Thickness
C1	DMF	0.5	No	5	9 μm
C2	DMF	0.5	Yes	5	
C3	acetone/DMF	0.5	Yes	5	
C4	acetone/DMF	0.25	Yes	8	

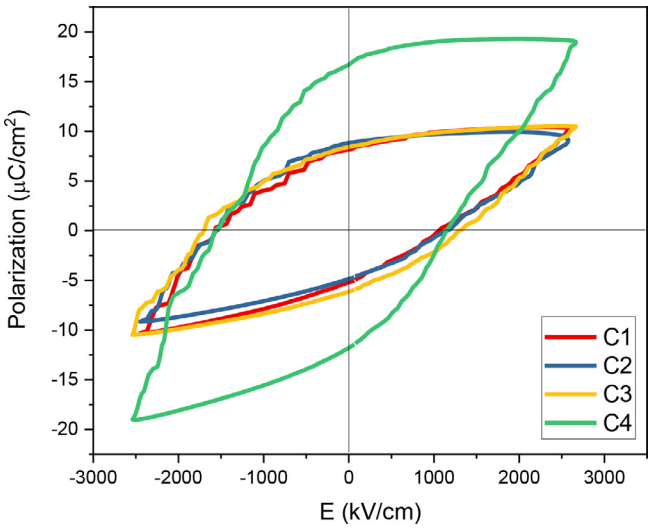

Fig. 3. Polarization loops of different conditions(C1–4) measured at a frequency of 5 Hz as a function of an applied electric field.

The finding suggests that films with almost the same piezoelectric properties can be made with a less toxic and costly solvent. On the other hand, the uniformity of the films may be affected by the solvent evaporation rate that will be discussed in the following section. Hence, using DMF/acetone solvent along with a low flowrate deposition of 0.25 ml/min led to a relatively high d_{33} value of 38 pm/V (C4). The d_{33} value is higher in comparison to the values observed in the literature [1,44].

To study the relationship between the deposition flowrate and thickness of the film, different samples were made with condition C4 but in 5 layers, resulted in films with the thickness of ~5 μm (C5). The obtained d_{33} value for these samples was even higher (d_{33} = 48 pm/V) than 9 μm thick samples. The corresponding polarization and strain loops of these samples are presented in Fig. 5, where the saturation and remnant polarization were 9.68 and 6.08 μC/cm^2, respectively. A possible reason for the positive effect of lower thickness on d_{33} value is the higher probability of the formation of aligned dipoles in lower thicknesses due to the mechanical stresses during the deposition process. Moreover, a higher number of layers can reduce the uniformity of films that can negatively affect the piezoelectric properties.

The average d_{33} value in the literature is between 13 and 34 pm/V for PVDF films [1,6,19,44–47], and 24–40 pm/V [1,44,48] for PVDF-TrFE films. The d_{33} value of PVDF films obtained in this work using the USC method was higher than the average d_{33} value of PVDF and PVDF-TrFE films. For comparison, the d_{33} values of some PVDF films made through various other methods in previous reports, are shown in Table 3. The comparison between d_{33} values reveals that the piezoelectric constant achieved in this work is higher than others reported in the literature. Moreover, in most other methods, the PVDF films had to be postprocessed with stretching, poling, quenching, and so forth. This is while the only post processing that performed on our samples was annealing at 100 °C.

3.2. X-ray diffractometry measurements

GIXRD measurements were performed using a CuKα target at 40 kV and 40 mA, with a step size of 0.01° at an incident angle of 0.55°. The XRD patterns in Fig. 6 exhibit two intense peaks overlapped at 2θ = 18.3°, corresponding to the α phase with (020) crystal plane and 2θ = 20.2° belonging to β phase with (110) crystal plane [15,16,50]. These planes are found in all of the samples, and they represent a higher proportion of the polar β phase, which brings about high piezoelectric properties in the films. The similarity of the XRD patterns for all the conditions shows that parameters such as ultrasonication, flowrate, and solvent evaporation

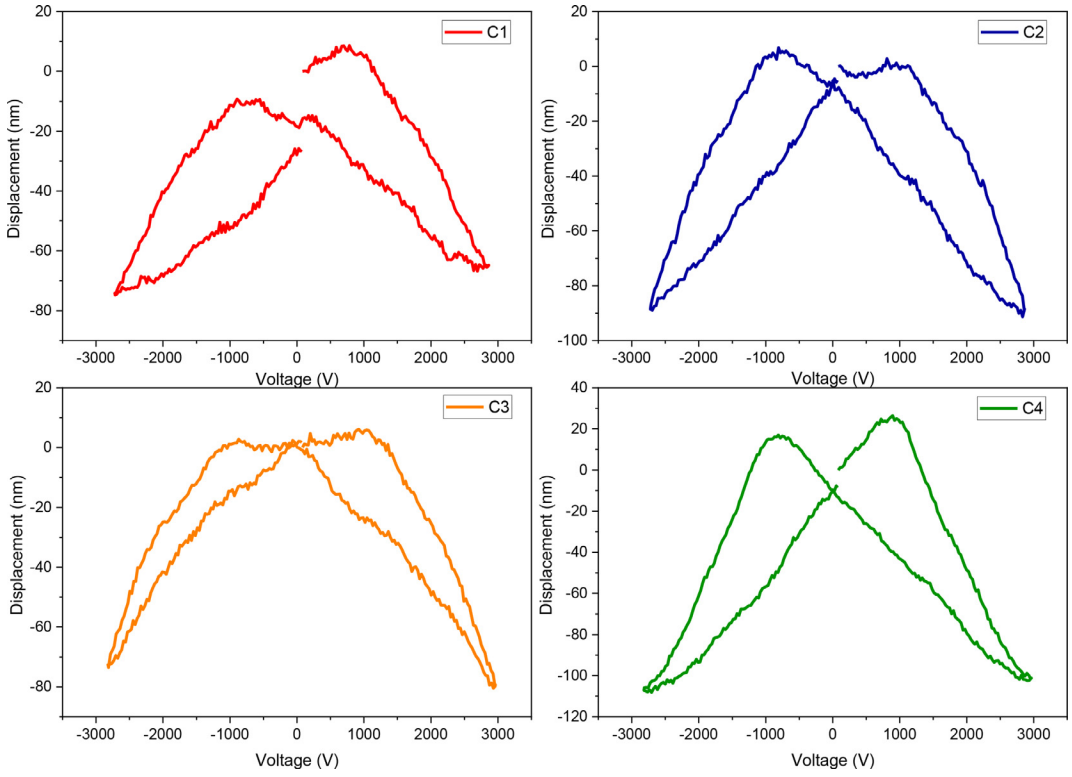

Fig. 4. Displacement-voltage (strain) loops for PVDF films made at conditions C1–4.

Table 2
Thickness and piezoelectric parameters of the samples made in different conditions(C1–4).

	No. of layers	Thickness (μm)	P_r (μC/cm^2)	P_s (μC/cm^2)	d_{33} (pm/V)	E_c (kV/cm)
C1	5	~9	8.2	10.4	23	1146
C2	5	~9	8.8	9.7	31	1258
C3	5	~9	8.4	10.5	28	1418
C4	8	~9	16.7	19.2	38	1272

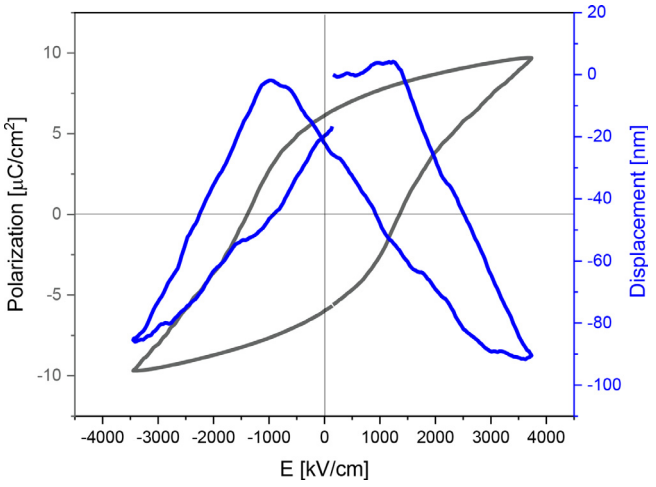

Fig. 5. Polarization and strain loops of C5.

rate, have not significantly altered the crystalline phase of the films. For further investigation, differential scanning calorimetry (DSC) measurements were also performed which will be discussed in the following section.

3.3. Differential scanning calorimetry (DSC) measurements

DSC thermal analyses were performed on samples fabricated in all conditions (C1–5). The heating curves are not shown in Fig. 7. The similarity between the melting temperature of PVDF films in α or β phases makes it difficult to unequivocally distinguish between these phases using the DSC data [15]. Nevertheless, DSC data can be used to determine between the formation of α/β and γ phase, within melting temperature ranges of 160–172 °C and 179–180 °C, respectively [15,51]. The endothermic peaks obtained in the heating curves at ~161 °C confirmed the existence of either α or β phase. Because of the ferroelectricity of the films, it can be concluded that β phase is the predominant phase in the measured samples [52–54].

Using DSC data, the degree of crystallinity of the samples was also calculated using the following equation [18]:

$$X_c(\%) = \left(\frac{\Delta H_m}{\Delta H_{m0}}\right) * 100 \quad (1)$$

where ΔH_m is the melting enthalpy of the sample and ΔH_{m0} is the melting enthalpy of a 100% crystalline PVDF film, equal to 103.4 J/g [18], when considering a 100% β phase PVDF film. All of the calculated crystallinities were around 56%, with no major differences between them.

Although both XRD and DSC measurements support the formation of β phase, the reason for the preferential formation of this phase in the spray coating method is not fully understood yet. According to Wang et al. [41], the reason can be attributed to the shear effect of radial outward capillary force and/or the interaction between the polar solvent and PVDF chain that causes local conformation changes and the nucleation of polar phase. On the other hand, Alluri et al. [55] suggested that high sound energy of the sonication in ultrasonic methods causes the formation of β polar phase, and therefore, the self-alignment of dipoles in the film. Some other works have also studied the vibrational stretching of molecular dipoles in PVDF solution which is induced by ultrasonication and transforms nonpolar α phase to β/γ polar phases [55].

Thus, ultrasonic spray coating helped to induce the β polar phase in our samples. However, as observed in the samples fabricated without ultrasonication (C1), annealing and stable conditions of the fabrication process still play an equally important role in the formation of β phase and the final properties of the films.

3.4. Uniformity and morphology of films

Surface morphology of the crystallized films was characterized by SEM, shown in Fig. 8, and by flattening AFM images using "SEM mode" in Gwyddion software, shown in Fig. 8. Although the temperature of processing may prominently influence the microstructure of the films [56], the goal of this study was to check the influence of the spraying process and precursor solution on uniformity and morphology. Accordingly, the annealing temperature was kept the same for all samples.

By comparing the surface morphology (Fig. 8) of samples fabricated with conditions C1 and C2 (without and with ultrasonication), it was observed that the size of pores was reduced with ultrasound. Yet, the AFM-morphology of grains changed a little as evidenced in Fig. 9. Changing the solvent to DMF/Acetone (70/30) for C3 reduced the number of pores compared to C1 and C2 in Fig. 8. Besides, the C3 film exhibited 3 different regions with slightly different morphologies and decreasing grain size (depicted as numbered circles 1, 2, and 3 in Fig. 9 for C3). Only region 1 was similar to the morphology in C1 and C2. Therefore, the mixture of DMF/acetone introduces the formation of different regions and

Table 3
Comparison of d_{33} value in different fabrication methods.

Ref.	Method	solution	thickness	Post processing	d_{33} (pm/V)
[45]	Casting	15 vol%	40 μm	Corona discharge poling at 250 MV/m	27
[46]	Aligned electrospinning	~18 wt%	–	–	27.4 ± 1.5
[6]	Spin coating	30 wt%	46 ± 2 μm	Quenching in liquid nitrogen, at the temperature of 77 K	~30
[22]	Electrospray deposition	0.05 wt%	400 ± 30 nm	Poling at max. 0.5 MV/m during deposition	43
[49]	3D printing	–	650 μm	Corona poling at 12 KV during deposition	0.048
[26]	Spray coating	2.4 wt%	8.5 μm	Corona poling, at 10 kV for 10 min	12
This work	Ultrasonic spray coating	5 wt%	5 μm	–	48

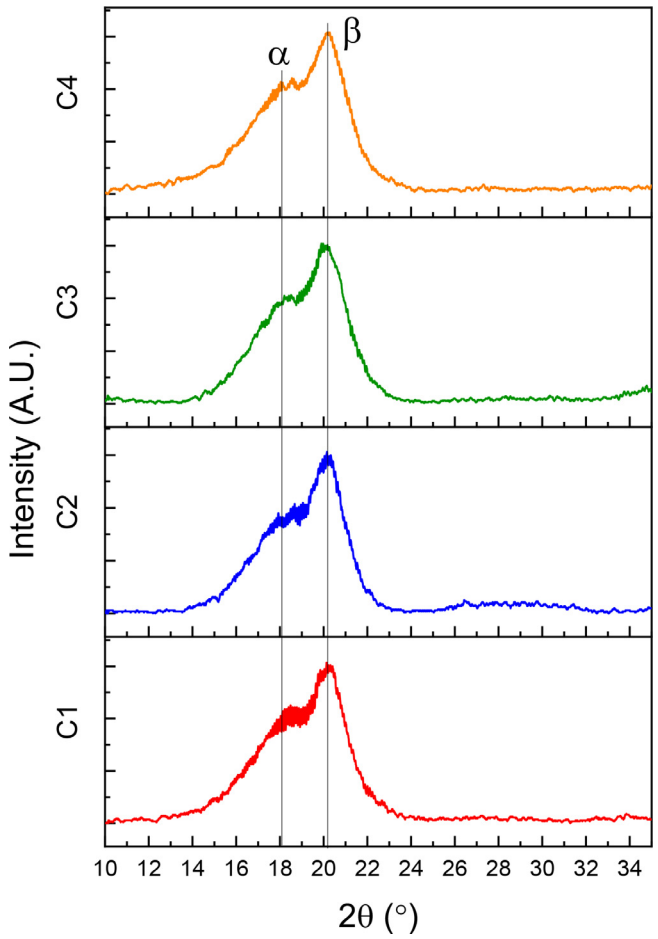

Fig. 6. GIXRD patterns of PVDF samples made with conditions C1–4.

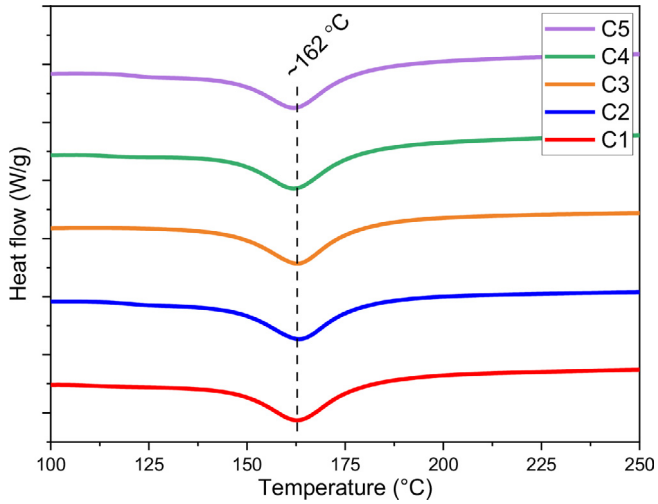

Fig. 7. DSC melting curves of PVDF films made with conditions C1–5.

morphologies. Finally, the reduction of the precursor solution flowrate also positively affected the surface morphology in terms of porosity of the layer (C4 in Fig. 8). Moreover, only regions 2 and 3 with small grain sizes appeared (C4 in Fig. 9). Consequently, comparing samples made in C4 (with DMF/Acetone (70/30) and lower flowrate) to the others, this particular processing condition produced notably less porous films. The same is true for a reduced number of layers (C5 in Fig. 9).

In addition to SEM, AFM studies were performed on the samples C1 to C5 in a scanning area of 10 × 10 μm shown in Fig. 10. As discussed in the previous paragraphs, samples C1 and C2 present similar morphologies with large grain sizes. Nevertheless, the RMS roughness calculated for C2 (deposited under ultrasonication) was almost a third lower than that of C1 (without ultrasonication). The use of DMF/acetone mixture as solvent had little effect on the roughness of C3 film, although it produced regions of different morphologies. The real impact was observed when a lower flowrate was employed (C4 and C5). Despite the different morphologies observed in Fig. 9, the roughness decreased even further as evidenced by the Z-scale and the RMS roughness values depicted in the corresponding images of Fig. 10.

Considering the piezoelectric measurements in Section 3.1, samples with higher piezoelectric coefficient have lower roughness values and more uniform surfaces. Roughness has an important influence on electrical [57] and thermal conduction [58]. Frictional temperature increases at microcontacts of rough surfaces [58]. However, this temperature rise should not cause any problem in room temperature applications, which is the environment our experiments have been performed in. Regarding the electrical conduction, surface roughness will cause excessive local electric fields at bumps [57], leading to lower piezoelectric responses and breakdown voltages. Moreover, lower porosity of the samples can decrease the value of leakage current [59]. Therefore, higher piezoelectric coefficient of the samples with higher surface quality can be explained by the absence of surface local electric fields and lower leakage current.

Both ultrasonication and the low flowrate of solution helped with the high surface quality of the films. A low flowrate provides less fluid to the tip at any given moment, which might cause the ultrasound to effectively produce smaller droplets. When such small droplets arrive at the substrate, films with less porosity and smaller roughness will be produced. Our results provide further support on the positive effect of ultrasonic spray coating along with a low flowrate deposition on the quality of pure PVDF films. They also highlight the significance of surface morphology control, low porosity and low surface roughness in the piezoelectric performance of PVDF films obtained by USC.

4. Conclusion

In this work, piezoelectric properties, morphology, and the crystalline phase of PVDF films produced using the nozzle-less ultrasonic spray coating method were studied. The results show that 5-layer deposition of 5 wt% PVDF in Acetone/DMF (30/70) solvent with a flowrate of 0.25 ml/min leads to films with outstanding piezoelectric properties (d_{33} = 48 pm/V) and good uniformity, without any need to perform common post-processing such as stretching or poling. This study confirms the significance of film uniformity for achieving highly piezoelectric films. The obtained d_{33} value, in the range of those usually obtained by expensive PVDF-TrFE films, brings us to the conclusion that USC method is capable of producing large-scale, low-cost, and high-quality piezoelectric films in one step. Likewise, USC allows the fabrication of flexible and wearable electronics with complex design and on different substrate materials, which expand its application to more innovative technologies. Thus, this is a promising method paving the way for the use of high quality pure PVDF films in the industry and large-scale engineering applications.

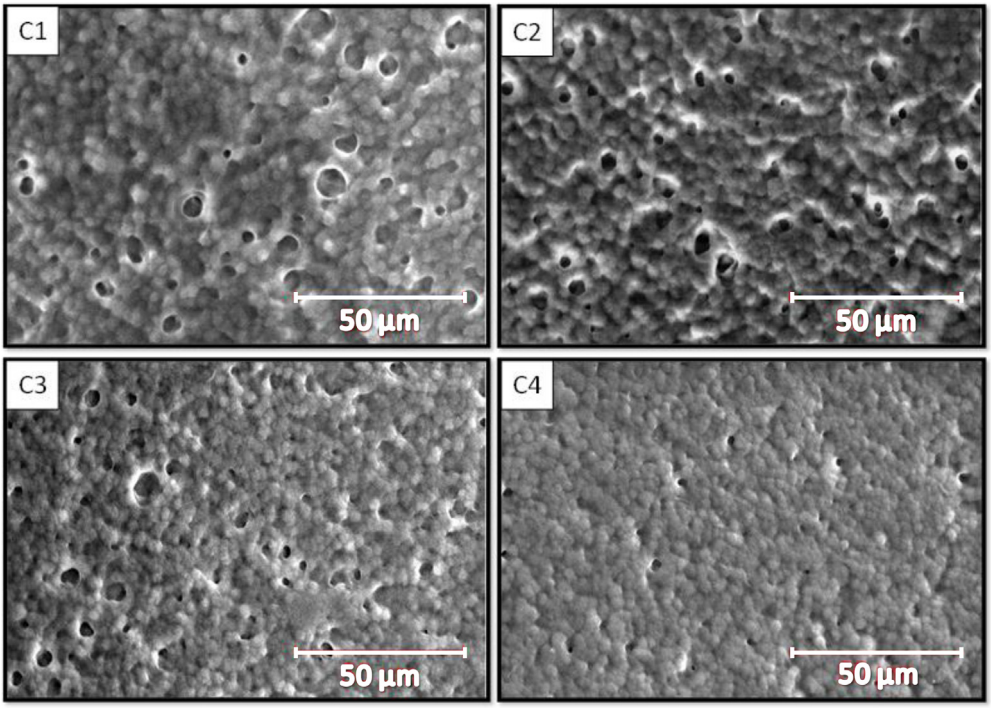

Fig. 8. SEM images from the of samples in condition C1–C4.

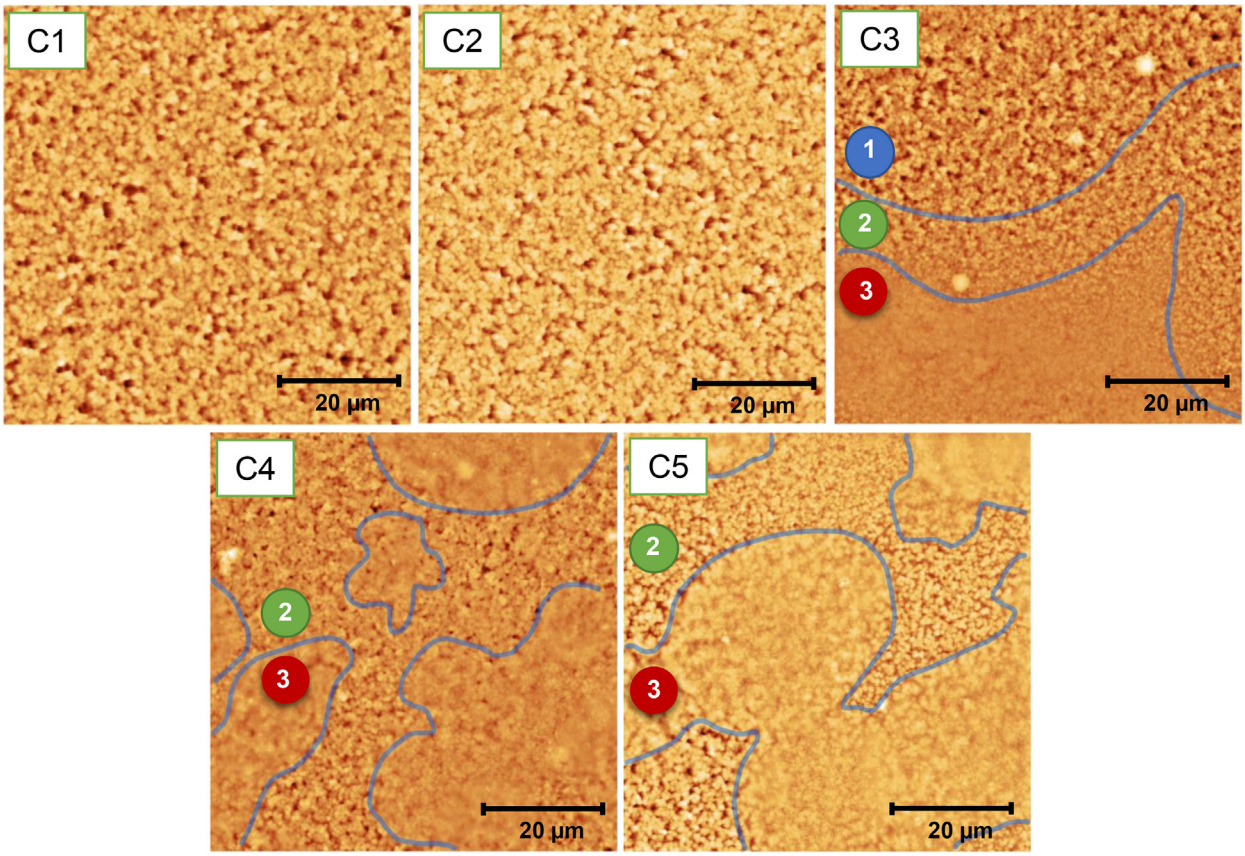

Fig. 9. AFM images of samples C1–C5 2D-rendered by "SEM mode" in Gwyddion AFM-analysis software.

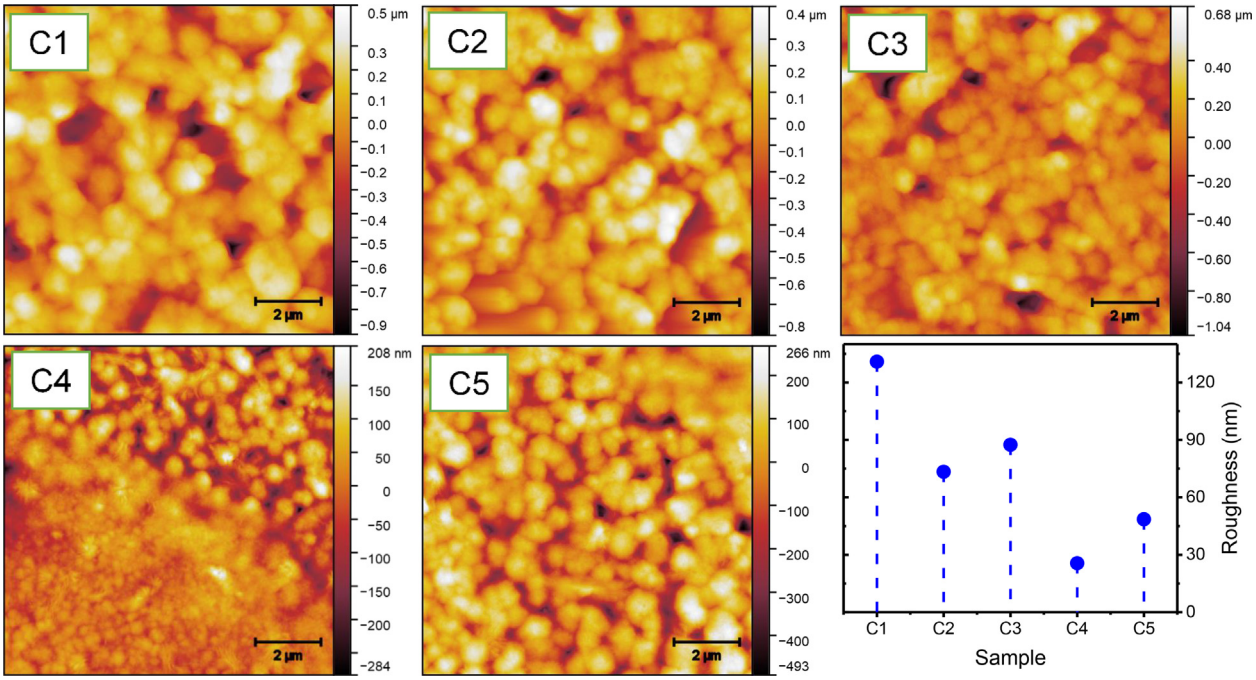

Fig. 10. AFM images of samples C1–C5. Also, estimated RMS roughness for the films made at different conditions.

5. Funding

This work was supported by the start-up grant of the FSE at the University of Groningen, the Netherlands; and MB thanks the support of the Postdoctoral CONACyT - Mexico scholarship (CVU 356403).

6. Data availability

The raw/processed data required to reproduce these findings are available from the corresponding author upon request.

Declaration of Competing Interest

The authors declare that they have no known competing financial interests or personal relationships that could have appeared to influence the work reported in this paper.

Acknowledgments

We gratefully acknowledge the invaluable support of Jacob Baas, Henk Bonder and Taraneh Mokabber in the lab. We also want to thank Beatriz Noheda for fruitful discussions.

References

[1] S. Mishra, L. Unnikrishnan, S.K. Nayak, S. Mohanty, Advances in piezoelectric polymer composites for energy harvesting applications: a systematic review, Macromol. Mater. Eng. 304 (2019) 1–25, https://doi.org/10.1002/mame.201800463.
[2] G.M. Sessler, Piezoelectricity in polyvinylidenefluoride, J. Acoust. Soc. Am. 70 (6) (1981) 1596–1608, https://doi.org/10.1121/1.387225.
[3] Y. Fu, E.C. Harvey, M.K. Ghantasala, G.M. Spinks, Design, fabrication and testing of piezoelectric polymer PVDF microactuators, Smart Mater. Struct. 15 (2006), https://doi.org/10.1088/0964-1726/15/1/023.
[4] Q.X. Chen, P.A. Payne, Industrial applications of piezoelectric polymer transducers, Meas. Sci. Technol. 6 (3) (1995) 249–267, https://doi.org/10.1088/0957-0233/6/3/001.
[5] R. Gregorio, Determination of the α, β, and γ crystalline phases of poly (vinylidene fluoride) films prepared at different conditions, J. Appl. Polym. Sci. 100 (4) (2006) 3272–3279, https://doi.org/10.1002/(ISSN)1097-462810.1002/app.v100:410.1002/app.23137.
[6] M. Fortunato, D. Cavallini, G. De Bellis, F. Marra, A. Tamburrano, F. Sarto, M.S. Sarto, Phase inversion in PVDF films with enhanced piezoresponse through spin-coating and quenching, Polymers (Basel) 11 (2019) 1–14, https://doi.org/10.3390/polym11071096.
[7] P.K. Szewczyk, A. Gradys, S.K. Kim, L. Persano, M. Marzec, A. Kryshtal, T. Busolo, A. Toncelli, D. Pisignano, A. Bernasik, S. Kar-Narayan, P. Sajkiewicz, U. Stachewicz, Enhanced piezoelectricity of electrospun polyvinylidene fluoride fibers for energy harvesting, ACS Appl. Mater. Interfaces 12 (11) (2020) 13575–13583, https://doi.org/10.1021/acsami.0c0257810.1021/acsami.0c02578.s001.
[8] M. Satthiyaraju, T. Ramesh, Nanomechanical, mechanical responses and characterization of piezoelectric nanoparticle-modified electrospun PVDF nanofibrous films, Arab. J. Sci. Eng. 44 (6) (2019) 5697–5709, https://doi.org/10.1007/s13369-018-03694-6.
[9] R. Guo, H. Zhang, S. Cao, X. Cui, Z. Yan, S. Sang, A self-powered stretchable sensor fabricated by serpentine PVDF fi lm for multiple dynamic monitoring, Mater. Des. 182 (2019) 108025, https://doi.org/10.1016/j.matdes.2019.108025.
[10] A. Nguyen, P. Sharma, T. Scott, E. Preciado, V. Klee, D. Sun, I.-H. Lu, D. Barroso, S. Kim, V.Y. Shur, A.R. Akhmatkhanov, A. Gruverman, L. Bartels, P.A. Dowben, Toward ferroelectric control of monolayer MoS2, Nano Lett. 15 (5) (2015) 3364–3369, https://doi.org/10.1021/acs.nanolett.5b00687.
[11] X. Wang, P. Wang, J. Wang, W. Hu, X. Zhou, N. Guo, H. Huang, S. Sun, H. Shen, T. Lin, M. Tang, L. Liao, A. Jiang, J. Sun, X. Meng, X. Chen, W. Lu, J. Chu, Ultrasensitive and broadband MoS2 photodetector driven by ferroelectrics, Adv. Mater. 27 (42) (2015) 6575–6581, https://doi.org/10.1002/adma.201503340.
[12] A. Laudari, J. Barron, A. Pickett, S. Guha, Tuning charge transport in PVDF-based organic ferroelectric transistors: status and outlook, ACS Appl. Mater. Interfaces 12 (24) (2020) 26757–26775, https://doi.org/10.1021/acsami.0c05731.
[13] Z. Wang, X. Wang, N. Zhao, J. He, S. Wang, G. Wu, Y. Cheng, The desirable dielectric properties and high thermal conductivity of epoxy composites with the cobweb-structured SiCnw–SiO2–NH2 hybrids, J. Mater. Sci.: Mater. Electron. 32 (16) (2021) 20973–20984, https://doi.org/10.1007/s10854-021-06543-9.
[14] X. Cai, T. Lei, D. Sun, L. Lin, A critical analysis of the α, β and γ phases in poly (vinylidene fluoride) using FTIR, RSC Adv. 7 (25) (2017) 15382–15389, https://doi.org/10.1039/C7RA01267E.
[15] P. Martins, A.C. Lopes, S. Lanceros-Mendez, Electroactive phases of poly (vinylidene fluoride): determination, processing and applications, Prog. Polym. Sci. 39 (4) (2014) 683–706, https://doi.org/10.1016/j.progpolymsci.2013.07.006.
[16] L.i. Li, M. Zhang, M. Rong, W. Ruan, Studies on the transformation process of PVDF from α to β phase by stretching, RSC Adv. 4 (8) (2014) 3938–3943, https://doi.org/10.1039/C3RA45134H.
[17] T. Lei, X. Cai, X. Wang, L. Yu, X. Hu, G. Zheng, W. Lv, L. Wang, D. Wu, D. Sun, L. Lin, Spectroscopic evidence for a high fraction of ferroelectric phase induced in

electrospun polyvinylidene fluoride fibers, RSC Adv. 3 (2013) 24952–24958, https://doi.org/10.1039/c3ra42622j.
[18] J. Gomes, J.S. Nunes, V. Sencadas, S. Lanceros-Mendez, Influence of the β-phase content and degree of crystallinity on the piezo-and ferroelectric properties of poly(vinylidene fluoride), Smart Mater. Struct. 19 (2010), https://doi.org/10.1088/0964-1726/19/6/065010.
[19] Y. Ting, N. Suprapto, K. Bunekar, Y.R.A. Sivasankar, Using annealing treatment on fabrication ionic liquid-based PVDF films, Coatings 10 (2020), https://doi.org/10.3390/coatings10010044.
[20] V.F. Cardoso, G. Minas, C.M. Costa, C.J. Tavares, S. Lanceros-Mendez, Micro and nanofilms of poly(vinylidene fluoride) with controlled thickness, morphology and electroactive crystalline phase for sensor and actuator applications, Smart Mater. Struct. 20 (2011), https://doi.org/10.1088/0964-1726/20/8/087002.
[21] W. Aik, M. Kotaki, Y. Liu, X. Lu, Morphology, polymorphism behavior and molecular orientation of electrospun poly (vinylidene fluoride) fibers, Polymer 48 (2007) 512–521, https://doi.org/10.1016/j.polymer.2006.11.036.
[22] I.B. Rietveld, K. Kobayashi, T. Honjo, K. Ishida, H. Yamada, K. Matsushige, Electrospray induced ferroelectricity in poly(vinylidene fluoride) thin films, J. Mater. Chem. 20 (2010) 8272–8278, https://doi.org/10.1039/c0jm01265c.
[23] Y. Li, W. Feng, L. Meng, K. Ming, Z. Li, L. Huang, Investigation on in-situ sprayed, annealed and corona poled PVDF-TrFE coatings for guided wave-based structural health monitoring: from crystallization to piezoelectricity, Mater. Des. 199 (2021) 109415, https://doi.org/10.1016/j.matdes.2020.109415.
[24] S. Hwangbo, J.M. Kang, G.T. Kim, Y.S. Jeon, K.S. Hwang, Direct formation of -poly(vinylidene fluoride) thin films by electrostatic spray deposition, J. Nanosci. Nanotechnol. 17 (2017) 7706–7710, https://doi.org/10.1166/jnn.2017.14821.
[25] M. Aleksandrova, Spray deposition of piezoelectric polymer on plastic substrate for vibrational harvesting and force sensing applications, AIMS Mater. Sci. 5 (2018) 1214–1222, https://doi.org/10.3934/matersci.2018.6.1214.
[26] H. Takise, M. Suzuki, T. Takahashi, S. Aoyagi, Film formation and characterisation of PVDF piezoelectric polymer thin film by spray coating and its application to helical spring, Int. J. Nanotechnol. 15 (2018) 900–913, https://doi.org/10.1504/IJNT.2018.099930.
[27] S.P. Sreenilayam, I.U. Ahad, V. Nicolosi, V. Acinas Garzon, D. Brabazon, Advanced materials of printed wearables for physiological parameter monitoring, Mater. Today 32 (2020) 147–177, https://doi.org/10.1016/j.mattod.2019.08.005.
[28] N.A. Shepelin, P.C. Sherrell, E. Goudeli, E.N. Skountzos, V.C. Lussini, G.W. Dicinoski, J.G. Shapter, A.V. Ellis, Printed recyclable and self-poled polymer piezoelectric generators through single-walled carbon nanotube templating, Energy Environ. Sci. 13 (3) (2020) 868–883, https://doi.org/10.1039/C9EE03059J.
[29] T. Siponkoski, M. Nelo, J. Palosaari, J. Peräntie, M. Sobocinski, J. Juuti, H. Jantunen, Electromechanical properties of PZT/P(VDF-TrFE) composite ink printed on a flexible organic substrate, Compos. Part B Eng. 80 (2015) 217–222, https://doi.org/10.1016/j.compositesb.2015.05.018.
[30] S. Bodkhe, G. Turcot, F.P. Gosselin, D. Therriault, One-step solvent evaporation-assisted 3D printing of piezoelectric PVDF nanocomposite structures, ACS Appl. Mater. Interfaces 9 (24) (2017) 20833–20842, https://doi.org/10.1021/acsami.7b0409510.1021/acsami.7b04095.s001.
[31] R. Gupta, K.D.M. Rao, K. Srivastava, A. Kumar, S. Kiruthika, G.U. Kulkarni, Spray coating of crack templates for the fabrication of transparent conductors and heaters on flat and curved surfaces, ACS Appl. Mater. Interfaces (2014), https://doi.org/10.1021/am503154z.
[32] N.A. Azarova, J.W. Owen, C.A. McLellan, M.A. Grimminger, E.K. Chapman, J.E. Anthony, O.D. Jurchescu, Fabrication of organic thin-film transistors by spray-deposition for low-cost, large-area electronics, Org. Electron. (2010), https://doi.org/10.1016/j.orgel.2010.09.008.
[33] C. Girotto, B.P. Rand, J. Genoe, P. Heremans, Exploring spray coating as a deposition technique for the fabrication of solution-processed solar cells, Sol. Energy Mater. Sol. Cells (2009), https://doi.org/10.1016/j.solmat.2008.11.052.
[34] H. Su, T.C. Jao, O. Barron, B.G. Pollet, S. Pasupathi, Low platinum loading for high temperature proton exchange membrane fuel cell developed by ultrasonic spray coating technique, J. Power Sources (2014), https://doi.org/10.1016/j.jpowsour.2014.05.086.
[35] A. Mahapatro, Metals for biomedical applications and devices, J. Biomater. Tissue Eng. (2012), https://doi.org/10.1166/jbt.2012.1059.
[36] A.M. Vilardell, N. Cinca, A. Concustell, S. Dosta, I.G. Cano, J.M. Guilemany, Cold spray as an emerging technology for biocompatible and antibacterial coatings: state of art, J. Mater. Sci. (2015), https://doi.org/10.1007/s10853-015-9013-1.
[37] S. Lin, H. Wang, X. Zhang, D. Wang, D. Zu, J. Song, Z. Liu, Y. Huang, K. Huang, N. Tao, Z. Li, X. Bai, B. Li, M. Lei, Z. Yu, H. Wu, Direct spray-coating of highly robust and transparent Ag nanowires for energy saving windows, Nano Energy (2019), https://doi.org/10.1016/j.nanoen.2019.04.071.
[38] I.S. Zope, S. Foo, D.G.J. Seah, A.T. Akunuri, A. Dasari, Development and evaluation of a water-based flame retardant spray coating for cotton fabrics, ACS Appl. Mater. Interfaces (2017), https://doi.org/10.1021/acsami.7b09863.
[39] R. Andrade, O. Skurtys, F. Osorio, Drop impact behavior on food using spray coating: fundamentals and applications, Food Res. Int. (2013), https://doi.org/10.1016/j.foodres.2013.07.042.
[40] A. You, M.A.Y. Be, I. In, Using ultrasonic atomization to produce an aerosol of micron-scale particles, Rev. Sci. Inst. 113301 (2005), https://doi.org/10.1063/1.2130336.
[41] S. Wang, Y. Liang, Transparent and ferroelectric poly (vinylidene fluoride) film achieved by simple ultrasonic spray coating method, Mater. Lett. 247 (2019) 71–74, https://doi.org/10.1016/j.matlet.2019.03.096.
[42] S. Tiwari, A. Gaur, C. Kumar, P. Maiti, Enhanced piezoelectric response in nanoclay induced electrospun PVDF nano fi bers for energy harvesting, Energy 171 (2019) 485–492, https://doi.org/10.1016/j.energy.2019.01.043.
[43] Q. Guo, G.Z. Cao, I.Y. Shen, Measurements of piezoelectric coefficient d33 of lead zirconate titanate thin films using a mini force hammer, J. Vib. Acoust. Trans. ASME 135 (2013) 1–9, https://doi.org/10.1115/1.4006881.
[44] K.S. Ramadan, D. Sameoto, S. Evoy, A review of piezoelectric polymers as functional materials for electromechanical transducers, Smart Mater. Struct. 23 (2014), https://doi.org/10.1088/0964-1726/23/3/033001.
[45] A.C. Lopes, J. Gutiérrez, J.M. Barandiarán, Direct fabrication of a 3D-shape film of polyvinylidene fluoride (PVDF) in the piezoelectric β-phase for sensor and actuator applications, Eur. Polym. J. 99 (2018) 111–116, https://doi.org/10.1016/j.eurpolymj.2017.12.009.
[46] C.M. Wu, M.H. Chou, W.Y. Zeng, Piezoelectric response of aligned electrospun polyvinylidene fluoride/carbon nanotube nanofibrous membranes, Nanomaterials 8 (2018) 1–13, https://doi.org/10.3390/nano8060420.
[47] P. Viswanath, H.-H. Huang, M. Yoshimura, Large piezoresponse in ultrathin organic ferroelectric nano lamellae through self-assembly processing, Appl. Surf. Sci. 532 (2020) 147188, https://doi.org/10.1016/j.apsusc.2020.147188.
[48] F. Narita, M. Fox, A review on piezoelectric, magnetostrictive, and magnetoelectric materials and device technologies for energy harvesting applications, Adv. Eng. Mater. 20 (5) (2018) 1700743, https://doi.org/10.1002/adem.v20.510.1002/adem.201700743.
[49] H. Kim, F. Torres, Y. Wu, D. Villagran, Y. Lin, T.-L. Tseng, Integrated 3D printing and corona poling process of PVDF piezoelectric films for pressure sensor application, Smart Mater. Struct. 26 (2017) 085027, https://doi.org/10.1088/1361-665x/aa738e.
[50] P.K. Mahato, A. Seal, S. Garain, S. Sen, Effect of fabrication technique on the crystalline phase and electrical properties of PVDF films, Mater. Sci. Pol. 33 (2015) 157–162, https://doi.org/10.1515/msp-2015-0020.
[51] N. Soin, D. Boyer, K. Prashanthi, S. Sharma, A.A. Narasimulu, J. Luo, T.H. Shah, E. Siores, T. Thundat, Exclusive self-aligned β-phase PVDF films with abnormal piezoelectric coefficient prepared via phase inversion, Chem. Commun. 51 (39) (2015) 8257–8260, https://doi.org/10.1039/C5CC01688F.
[52] B. Mahale, D. Bodas, S.A. Gangal, Study of β -phase development in spin-coated PVDF thick films, Bullet. Mater. Sci. 40 (2017) 569–575, https://doi.org/10.1007/s12034-017-1390-4.
[53] W. Ma, J. Zhang, X. Wang, Crystallizaion and surface morphology of poly (vinylidene fluoride)/poly(methylmethacrylate) films by solution casting on different substrates, Appl. Surf. Sci. 254 (10) (2008) 2947–2954, https://doi.org/10.1016/j.apsusc.2007.10.037.
[54] S. Lanceros-Méndez, J.F. Mano, A.M. Costa, V.H. Schmidt, FTIR and DSC studies of mechanically deformed β-PVDF films, J. Macromol. Sci. – Phys. 40B (2001) 517–527, https://doi.org/10.1081/MB-100106174.
[55] N.R. Alluri, A. Chandrasekhar, J.H. Jeong, S.-J. Kim, Enhanced electroactive β-phase of the sonication-process-derived PVDF-activated carbon composite film for efficient energy conversion and a battery-free acceleration sensor, J. Mater. Chem. C 5 (20) (2017) 4833–4844, https://doi.org/10.1039/C7TC00568G.
[56] M. Li, I. Katsouras, C. Piliego, G. Glasser, I. Lieberwirth, P.W.M. Blom, D.M. de Leeuw, Controlling the microstructure of poly(vinylidene-fluoride) (PVDF) thin films for microelectronics, J. Mater. Chem. C 1 (2013) 7695, https://doi.org/10.1039/c3tc31774a.
[57] P. Zhang, Effects of Surface Roughness on Electrical Contact, RF Heating and Field Enhancement, 2012.
[58] S. Wang, K. Komvopoulos, A fractal theory of the interfaoial temperature distribution in the slow sliding regime: Part I—Elastic contact and heat transfer analysis, J. Tribol. 116 (1994) 812–822, https://doi.org/10.1115/1.2927338.
[59] M.B. Suresh, T.-H. Yeh, C.-C. Yu, C.-C. Chou, Dielectric and ferroelectric properties of polyvinylidene fluoride (PVDF)-Pb0.52Zr0.48TiO3 (PZT) nano composite films, Ferroelectrics 381 (1) (2009) 80–86, https://doi.org/10.1080/00150190902869699.